On the controllability assessment of biofeedback eyeglasses used in Presbyopia treatment☆

Germán Yamhure, Arturo Fajardo *, C.I. Paez-Rueda, Gabriel Perilla, Manuel Pérez

Department of Electronic Engineering, Pontificia Universidad Javeriana, Calle 40 No. 5-50. Ed. José Gabriel Maldonado S.J., 4to piso, Bogotá D.C. 110311, Colombia

ARTICLE INFO

ABSTRACT

In recent years, hybrid biofeedback systems utilizing user-controlled electrically tunable lenses have emerged as potential treatments for presbyopia. However, the controllability of these systems, closely linked to user adaptability, has received limited attention in the literature due to the challenges associated with obtaining a comprehensive system model. In this study, we present the design, implementation, and validation of an innovative experimental setup aimed at researching and evaluating the controllability of such a biofeedback system. Our setup incorporates a novel low-complexity model, considering the brain, natural lenses (e.g., the crystalline lens), and electrically tunable lenses, to establish a fundamental model for hybrid biofeedback systems. This model is developed based on an analysis of biofeedback systems, geometrical optics, and control theory, facilitating the identification of strategies to decouple system dynamics and enable precise controllability analysis. The proposed experimental setup was validated with volunteers, providing evidence that confirms the reliable operation of the biofeedback system. Our approach encourages a shift from conventional qualitative approaches toward quantitative evaluation of biofeedback devices. The proposed model and experimental setup hold the potential to statistically assess the controllability of hybrid biofeedback systems for correcting presbyopia, paving the way for further advancements in this field.

1. Introduction

Presbyopia, a prevalent clinical condition, affects an estimated 1.8 billion individuals worldwide, manifests as a loss in the eye's ability to adjust its refractive or optical power, typically within a few diopters [1–3]. Presbyopia can be partially corrected through the utilization of a diverse range of optical devices and methodologies [4]. These include multifocal corrective eyeglasses, monovision, and multifocal contact lenses, as well as smart autofocusing wearable eyeglasses [4–10].

In conventional approaches utilizing lenses with fixed optical power, the patient's dynamic range is expanded, thereby enabling them to focus at various distances through the resulting biofeedback system [1]. For instance, bifocal eyeglasses incorporate lenses with two distinct optical powers, and the patient can select the desired focal region by adjusting the angle of the craniocervical area and tilting their eyes [11], as illustrated in Fig. 1(a). In this biofeedback system, the person actively engages their muscles by alternately relaxing and contracting them to elicit the desired effect [12]. However, certain individuals face challenges in utilizing these methods due to inherent limitations of the eyes, such as disparity vergence [13], or encounter difficulties in adapting to these approaches [14].

Smart autofocusing wearable eyeglasses, utilizing large aperture variable-focus lenses [15], have emerged as a promising solution for correcting presbyopia [4–9]. The conventional approach for achieving automatic lens accommodation in smart eyeglasses is to calculate the required optical power based on the distance (d) between the eyeglasses and the object to be focused, as shown in Fig. 1(b). This distance can be measured directly using time-of-flight sensors [4,6,7] or indirectly by tracking the person's eye movements [5,8,9], both of these measurement techniques are shown in Fig. 1(b). The first method requires that the object reflects a strong signal to be detected by the sensor's transducer. Consequently, if the person intends to view objects with low reflectivity (e.g., thin cloth or smoke), this approach limits the ability to achieve correct focus on the object. To overcome this limitation, the second approach utilizes vergence to calculate the distance between the eyeglasses and the object. In this method, a sensor such as a camera is employed to determine the convergence angle (ϕ in Fig. 1(b)). These systems require an initial calibration procedure in which the person directs their attention to an object at a predetermined distance. Following this calibration phase, the system regulates the
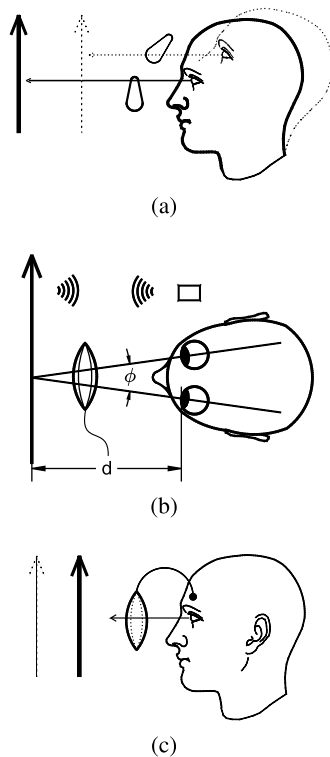

Fig. 1. Presbyopia correction paradigms with eyeglasses. (a) Systems based on biofeedback and fixed optical power devices. (b) Systems based on distance measurement and electrically tunable lenses. (c) Systems based on biofeedback and controlled optical power devices.

optical power of the external lens based on the measured distance between the object and the eyeglasses, assuming a constant optical power of the internal lens. Consequently, the prolonged utilization of such eyeglasses may result in fatigue of the ciliary muscles, as their activity remains nearly constant over an extended duration. This phenomenon closely resembles computer vision syndrome, characterized by ocular strain and discomfort [16]. It is noteworthy that although directly measuring this phenomenon can be challenging, there are various estimation methods available for assessment [17,18]. Moreover, in accordance with the Helmholtz–Hess–Gullstrand and Donders–Duane–Fincham theories of presbyopia, the fatigue and discomfort experienced during the extended usage of these eyeglasses could be intensified in individuals with presbyopia.

The Helmholtz–Hess–Gullstrand theory attributes the loss of accommodation in presbyopia solely to the morphological changes in the crystalline lens capsule [19]. Conversely, the Donders–Duane–Fincham theory assigns the age-related decline in accommodation exclusively to the biomechanical properties of the ciliary muscles [19]. According to both theories, as individuals experience a reduction in accommodation, greater effort from the ciliary muscles is required to achieve the same change in optical power. To illustrate this, let us explore the examples discussed below. Based on the Helmholtz–Hess–Gullstrand theory, assuming a dynamic range of 15 diopters (D) during childhood with a linear relationship to the mechanical strength of the muscles, maximum muscle contraction would be needed at 15D. However, as the dynamic range diminishes to only 1D with age, the ciliary muscles must exert the same level of effort as during childhood to accommodate the lens from 14D to 15D, resulting in maximum muscle contraction. In the case of the Donders–Duane–Fincham theory, if the crystalline lens maintains its dynamic range of 15D, the mechanical strength required exceeds that of childhood due to muscle degradation. In both models, the use of an external lens in smart autofocusing wearable eyeglasses

improves overall optical power while reducing strain on the ciliary muscle. However, it is important to note that in these eyeglasses, the optical power of the crystalline lens remains relatively constant. As a result, prolonged exertion of the ciliary muscle could result in eye fatigue, impacting individuals with both normal vision and presbyopia. To alleviate this fatigue, it is recommended to engage in relaxing exercises such as yoga [20] or employ an external lens with variable optical power controlled by the person or an automated system. This enables the adjustment of the optical power to achieve focus and relax the associated eye muscles.

In recent advancements within the field of presbyopia correction, a novel approach has emerged that utilizes Electromyography signals (EMG) to control eyeglasses [10]. This innovative biofeedback system offers promising potential for alleviating eye fatigue, particularly ciliary muscle fatigue, by empowering persons to regulate the optical power of their eyeglasses. By exerting control over the internal lens's optical power and subsequently inducing relaxation in the ciliary muscles, individuals can effectively mitigate the strain experienced. Nevertheless, the validation of this prototype primarily relied on subjective person perception tests, with crucial aspects such as the controllability of the biofeedback system left unexplored by the researchers. The controllability of a biofeedback system is a key factor in determining its acceptance, as demonstrated by studies on biofeedback systems that integrate progressive or bifocal lenses [13,14]. Currently, the assessment of a biofeedback system's performance is limited to subjective tests that fail to capture the person's perception of its controllability. The absence of objective information poses significant challenges for biofeedback system designers. Therefore, an important unresolved question in this field relates to the objective measurement of controllability and individual adaptability in such systems.

To the best of the authors' knowledge, no previous study has been conducted on the controllability of this problem. This could be attributed to the lack of a comprehensive model for the biofeedback system, which poses challenges in analyzing its controllability. However, there have been relevant works focusing on modeling the eye's biological system. For example, the modeling of neurological control of accommodation involves a static model that relates the accommodative response to the accommodative stimulus [21]. Furthermore, this modeling approach has recently been employed to enable users to control their autofocusing wearable eyeglasses devices [22]. The procedure involves conducting experiments where patients manually adjust the optical power of tunable lenses in response to changes in the distance to the observed object and lighting conditions.

This article presents an experimental method to investigate and assess the controllability of the biofeedback system described in [10]. We propose a strategy similar to that suggested by [22], with the additional consideration of maintaining constant distance and illumination conditions. This approach aims to reduce the number of variables involved and mitigate their influences, such as variations in pupil aperture. In both approaches, the subject has control over the optical power of external lenses. However, it should be noted that the validation of the model in [22] relies on subjective individual evaluations (such as the Snellen test) rather than objective measurements. The proposed experimental setup, allows for the independent adjustment of each lens within the cascade of lenses, including the camera and the cornea-lens system. This setup, depicted in Fig. 6, comprises the EMG Controlled Image System (CIS), the Image Projection System (IPS), the EMG system, and the Study Participant (SP). The results demonstrate that, following a brief training period, all volunteers were able to manipulate the camera's focus to enhance image sharpness in the image projection system. The contributions of this paper are as follows:

- Development of a test and experimental setup to evaluate the controllability of biofeedback systems using electrically tunable lenses.
- Designing an experiment to isolate specific physical variables in complex biofeedback systems with electrically tunable lenses.
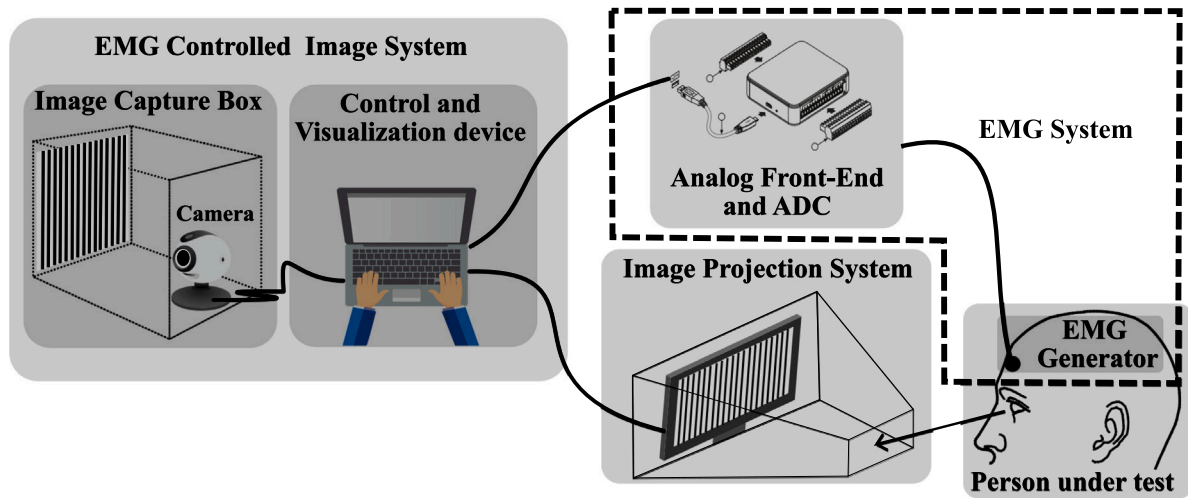
Fig. 2. Block diagram of the proposed system.

• Proposing a simplified brain control scheme for optical power devices.
• Introduction a novel taxonomy for the learning, teaching, and evaluation of biofeedback systems.

The paper is structured as follows: Section 2 introduces a simplified optical model of the system proposed in [10] and presents a novel taxonomy of biofeedback systems using a concise theoretical framework. In Section 3, the details of the experimental setup and methods employed in this study are presented. The experimental findings are summarized in Section 4, followed by a discussion on the limitations of this work. Finally, Section 5 presents the conclusions drawn from the study and outlines future research directions.

2. Biofeedback system modeling

2.1. A brief description of optics in human vision

The person's accommodation capacity refers to their ability to adjust the curvature of their crystalline lenses using the activity of their ciliary muscles, which determines the dynamic range of optical power. This ability allows them to form a clear image of the desired object on the retina. In cases where the accommodation capacity is insufficient, external lenses can provide assistance.

A conventional system utilized for correcting refractive errors of the eye comprises an external lens and the internal eye lenses, along with their associated muscles. Fig. 3 illustrates a simplified optical model of this system, while Fig. 3(a) presents its schematic representation, and Fig. 3(b) displays its first-order optical model. Considering that the cornea has a fixed optical power and that only the lens has accommodation capacity, this system is modeled as a single internal lens called L_2. Using this model for positive lenses, the external lens (L_1) creates a virtual image at a greater distance from the L_2 reference plane (i.e., $S_1 > S$). This virtual image is focused by two lenses on the retina, which is located at a distance of S'_1. If lens L_1 is removed from the correction system, the resulting lens system (i.e., crystalline-cornea) will produce an image S' from L_2. As a result, this image is created behind the retina, and the person sees a blurred image of the object. The optical power (P) of L_1 required to create an image on the retina is given by [23]:

$$P = \frac{1}{-S_1} - \frac{1}{S},$$ (1)

where P is given in diopters and S_1, S are given in meters. Despite its simplicity, this model provides insights into various phenomena associated with human vision. For example, this model allows quantitatively
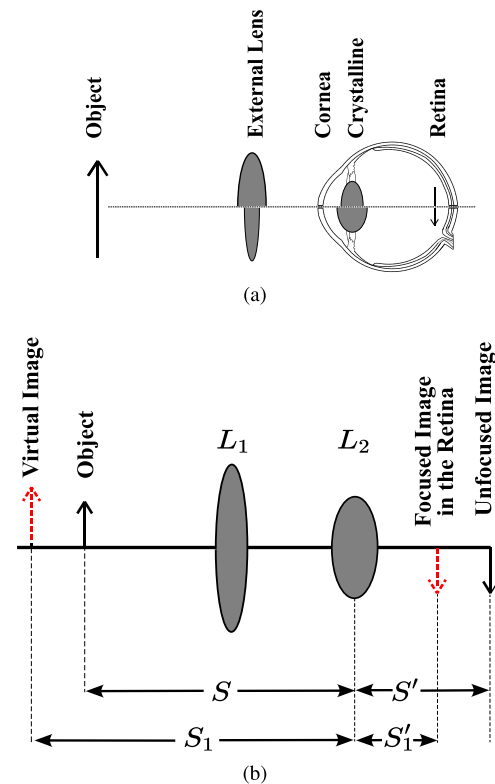

Fig. 3. The simple optical system of human vision. (a) Scheme of the system. (b) First-order optical model.

determining (using the maximum optical power of the lens L_2 and S'_1) the minimum distance to the object necessary to guarantee a sharp image. Additionally, it also explains why a person with presbyopia should move objects away to improve image sharpness or how the SP can create the image without moving the object by using an external lens. Furthermore, whether an individual has this condition or not, wearing L_1 with user-controlled optical power can potentially reduce the optical power of L_2 by relaxing the ciliary muscle and alleviating eyestrain (asthenopia) associated with prolonged focusing on objects, such as when working in front of a computer for extended periods. In this context, the user has the ability to adjust the ciliary muscles and modify the optical power of the external lens to suit their needs.

The combined optical power of the eye lens and the external lens must match the required power to form a clear image on the retina. This holds true even when considering the aperture adjustment of the pupil, as mentioned in [24].

Whether the object is moving closer or farther away, the described cascade optical system offers two simple solutions to create the image on the retina. The first approach involves keeping the optical power of the external lens constant while adjusting the optical power of the crystalline lens. The second option is to fix the power of the crystalline lens and vary the power of the external lens. However, there are infinite combinations of external lens and crystalline lens powers that can be utilized to form an image on the retina.

In this context, the use of bifocal and progressive lenses is widely employed, enabling individuals to achieve appropriate focus by combining different zones of the external lens with varying optical powers and the optical power of the crystalline lens, as illustrated in Fig. 1(a). To enhance image sharpness, individuals can adjust the tilt of their head (craniocervical angle) and the elevation and depression of their eyes. This exemplifies the concept of biofeedback, which involves muscle control, such as the rectus muscles of the eye.

It is important to note that achieving a sharp image on the retina involves a combination of the optical power of the crystalline lens and the opening of the pupil. Furthermore, the model under discussion does not account for the well-known Depth-of-Field (DoF) phenomenon, which defines the range of distances between the lens and the object that result in an image without noticeable blur [21]. The DoF is closely related to depth focus, which quantifies the range of optical power variations in the lens that produce imperceptible changes in blur. While the geometric optics model suggests a single distance known as the hyperfocal distance, the limited resolution of the retina leads to a range of distances, even within the foveal region. Increasing the aperture of the pupil allows more light rays to reach the retina, which can influence the perception of blur. Conversely, pupil constriction expands the DoF, aligning the behavior of the eye's lens system more closely with that of a pinhole camera, which has an infinite DoF.

2.2. Brief biofeedback framework

The concept of biofeedback finds wide application in various domains, including rehabilitation, sensory substitution, augmented reality, and sports training [10]. Due to its multi-dimensionality, the concept of biofeedback has yielded several definitions. On the one hand, the authors in [10] define biofeedback as a process that allows a person to learn to change their physiological activity in order to improve their health and performance. On the other hand, biofeedback is defined in [25] as the process of becoming aware of various physiological functions in order to voluntarily manipulate them at will. This process is developed using instruments that provide information about those functions (e.g., electromyography, skin temperature, heart rate, blood pressure, brain waves, etc.) Finally, in [26], biofeedback is defined as a control system related to the human body that operates on two elements: a natural and an artificial biofeedback mechanism. Natural biofeedback is described as a mechanism for regulating the human body's functioning. Artificial biofeedback is presented as a control system equipped with sensors that alert the person to interact with some natural regulatory mechanism controlled by the brain.

Inspired by the human nervous system and the aforementioned biofeedback definitions, we propose a comprehensive biofeedback-system information-flow diagram, as depicted in Fig. 4. The diagram elucidates the afferent flow, which represents the information flow from peripheral elements (e.g., organs, muscles, external objects) to the control unit (i.e., the brain). Conversely, the efferent information flow is defined as the flow from the control unit to the periphery elements. Within this diagram, an efferent action or information flow is represented by arrows labeled as EIn (Efferent Internal-nth) or EEn (Efferent External-nth), while afferent actions or information flows
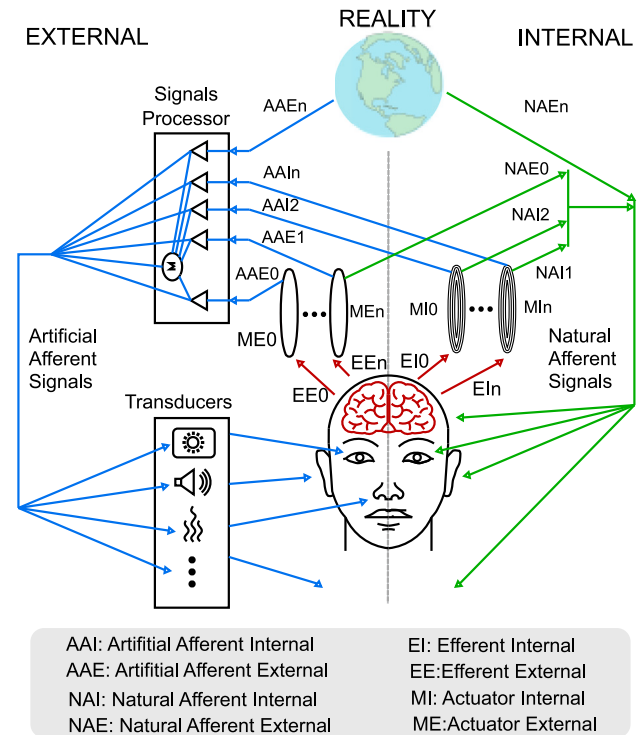

Fig. 4. Block diagram of information flow in biofeedback systems.

are illustrated by arrows labeled as AAIn (Artificial Afferent Internal-nth), AAEn (Artificial Afferent External-nth), NIn (Natural Afferent Internal-nth), and NAEn (Natural Afferent External-nth).

The proposed biofeedback diagram serves as a valuable tool for understanding the diverse contexts in which biofeedback is applied. For instance, it elucidates the information flow required to perceive the external environment, referred to as "REALITY" in Fig. 4. This perception is achieved through afferent information flow from the human senses to the brain. Another example involves the process of picking up an object, where the brain controls the action through efferent and afferent actions generated by feedback and learning mechanisms. Specifically, the brain activates the appropriate muscular system to move the hand in a specific direction (efferent action), while muscle spindles provide proprioception information, indicating the hand's position at each moment in time (efferent action). Consequently, the brain successfully accomplishes the task of picking up the object. Moreover, in the context of enhancing the learning process of fine motor skills in highly competitive athletes, muscular activity is captured using a signal processor, such as electromyography (EMG). This captured information is presented to the athlete via a screen (external afferent information flow), allowing them to perceive and interpret the information visually (internal afferent information flow). The athlete utilizes this information to adjust and refine their muscle movements (external afferent action). As a result of such biofeedback-driven training, athletes experience improvements in their performance.

By analyzing the proposed diagram and relevant literature, we proposed a taxonomy that categorizes various types of biofeedback, which is summarized in Table 1. Additionally, the table highlights applications associated with each type of biofeedback.

2.3. Modeling of the brain control involved in biofeedback systems based on electrically tunable lenses

This study presents a modeling approach to understand the brain control involved in biofeedback systems utilizing electrically tunable

Table 1
A simple taxonomy of biofeedback types.

Biofeedback type	Afferent flow	Efferent flow	Application examples
Natural	Internal	Internal	Natural blood glucose control [26]
Afferent Artificial	External	Internal	1. Rehabilitation of Motor Function [27–32] 2. Breathing control as a mechanism for controlling muscular stress [33,34]
Efferent Artificial	Internal	External	Blind people use canes to navigate their surroundings [35]
Fully Artificial	External	External	Virtual reality games [36,37].
Hybrid	Internal and/or External		1. Internal-afferent and external–internal efferent flow: use of EMG-controlled optical power lenses. [4–9] 2. Afferent and efferent flow both internal and external: Insulin pump to help with blood glucose control [26].
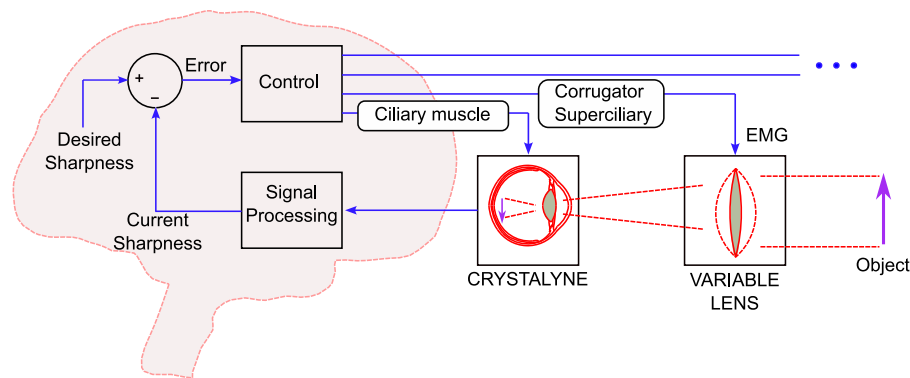
Fig. 5. Simplified brain control model for electrically tunable lenses.

lenses to achieve sharp image projection onto the retina. The eyeglasses biofeedback systems based on distance measurement and controlled optical power devices (shown in Fig. 1(b)) establish the optical power of the external lens (i.e., L1 in Fig. 3(b)). As a natural biofeedback system, the user can intervene by adjusting the line of sight and vergence. However, the external device determines the vergence distance and calculates the optical power of the external lens, thereby denying the user any degree of control over the optical power of the crystalline lens. Consequently, the user must adapt to the external device's settings. Under this approach, the optical power of the crystalline lens (i.e., L2) is almost constant. The proposed system shows a distance estimation error that the user can correct by changing the optical power of the lens until the desired sharpness is achieved. As a result, this feedback system is natural (as defined in Table 1) and it is assumed to be perfectly stable. In addition, as we discussed in Section 2.1, a variety of lens optical power combinations (i.e., L1 and L2) could produce a sharpness image in eyeglasses biofeedback systems that do not require distance measurement. In these systems, the user can control the optical power of the external lens (i.e., L1) by inclining the neck (and eyes) or modifying the myoelectric activity of a muscle (e.g., corrugator superciliary muscle [10]), as shown in the Figs. 1(a) and 1(c). The user can also adjust the optical power of the crystalline lens (i.e., L2). As a result, this biofeedback system is a hybrid one (as defined in Table 1), and its controllability cannot be guaranteed. Furthermore, there is some evidence of some people's inability to adapt to the use of eyeglass biofeedback systems based on bifocal and progressive lenses (i.e., the system shown in Fig. 1(a)) [14]. It is crucial to recognize the importance of a functional model for analyzing the controllability of the system. This compact model aids in determining the optical power of the external lenses in the presbyopia correction system that utilizes tunable lenses. However, it should be noted that with the proposed model and its experimental setup, it is not possible to evaluate the system's controllability because the brain control involved in the proposed setup is not considered.

In our literature review, we have identified a limited number of studies that have addressed the modeling aspect of presbyopia correction systems using tunable external lenses. One notable example is the work by [22], where they propose an experimental setup allowing patients to manually control the optical power of external lenses. The Snellen test is employed to assess visual acuity, considering variations in distance and lighting conditions. Based on the obtained results, the authors develop individual-specific compact empirical models of subjective accommodative error based on the model proposed in [38]. This compact model aid in determining the optical power of the external lenses in the presbyopia correction system utilizing tunable ones. However, it should be noted that, to the best of our knowledge, this particular model does not facilitate the evaluation of the system's controllability. Furthermore, it is crucial to recognize the importance of a functional model for analyzing the controllability of the system.

To address the modeling gap identified, we propose a simplified model of smart eyeglasses based on tunable lenses. In this proposed model, the output variable of the human vision system can be defined as image sharpness, which is influenced by several factors [39,40]:

- Multiple actuators, such as the muscles associated with the optical power control of the involved lens (e.g., crystalline and external lens), the rectus muscles of the eye, the muscles associated with pupil opening and closing, and the muscles associated with changes in the axial length of the eyeball [40], among others, play a role in the biofeedback system.
- External factors, such as the speed of object movement, image contrast, ambient lighting, and other variables detected by the system, can modify its functionality.
- A powerful control system (i.e., the brain) stands out for its remarkable plasticity and learning capacity. It controls the various actuators involved and analyzes data from related sensors to achieve the desired sharpness. Additionally, the control actions are directly influenced by the individual's intention, such as focusing on a specific object in a scene.

The simple model, shown in Fig. 5, allows comprehension of the eyeglasses system proposed in [10]. This model only takes into account two sharpness control loops and the main system actuators (Ciliary

muscle and Corrugator Superciliary). Despite the significant simplifications, the model reflects the operational complexity of the control brain as well as the fact that the system has an infinite number of solutions.

2.4. On the objective assessment of electrically tunable eyeglasses' controllability

The Snellen test is used to determine the required optical power in the traditional approach to improving human vision with eyeglasses. This test involves an examiner changing the external lenses and receiving feedback from a patient on the sharpness perception of projected letters and symbols of varying sizes. Therefore, the obtained result may contain significant biases due to subjective assessment of sharpness, for which the examiner confirms the person's ability to identify the symbols. This check helps to reduce the bias introduced by the patient. However, to avoid test subjectivity, the user's assessment must be removed.

Given the enormous difficulty of obtaining a system model and the desire to analyze the controllability of the biofeedback system proposed in [10], one possible approach is to implement a platform that decouples the control of the external lens from the other actuators involved in image focusing (primarily the crystalline lens) under controlled conditions. The design goals of this type of platform are as follows:

- Maintain a constant distance between the user and the observed object.
- Control the lighting environment to keep the pupil opening almost constant.
- Keep the eyes in the same relative position to the object to avoid vergence.
- Limit saccadic movements by avoiding the presence of points of greater attention using a spatially and static projected image.
- Limit peripheral vision to avoid user distractions.
- Minimize the impact of varying pupil apertures by maintaining almost constant lighting conditions.

To meet this challenge, we propose the platform depicted in Figs. 2 and 6. This experimental setup will be explained in detail in Section 3.2.

3. Proposed biofeedback system

3.1. A brief restrictions context

As explained in [21], the sensory and motor pathways responsible for blur-driven accommodation constitute a complex process. This process involves the contraction of the ciliary muscles, which modifies the shape of the crystalline lens based on the image projected onto the retina. Accommodation encompasses several components, including reflex, vergence, proximal, and tonics, which incorporate subjective perception, experiential appraisals, and other brain processes. Consequently, the control of external lenses based on neurological signals remains an ongoing challenge due to the inherent complexity involved. To mitigates the need for brain–computer interfaces, the direct brain control has been replaced in some smart eyeglasses implementations by alternative methods such as measuring the distance between the user and an object or utilizing the EMG signal from a facial muscle to regulate the optical power of the external lenses [4–10].

In [10], the authors utilize a signal processing strategy to monitor the activity of the superciliary corrugator muscle for regulating the power of external lenses, rather than relying on direct brain control. This approach is commonly employed in biofeedback systems. A classic example of this concept is the control of a computer mouse, where the user's brain serves as a direct controller of hand muscles, indirectly affecting the cursor's position on the screen. The superciliary corrugator muscle (along with neighboring muscles) is frequently engaged during visual tasks and it is known to contribute to the improvement of
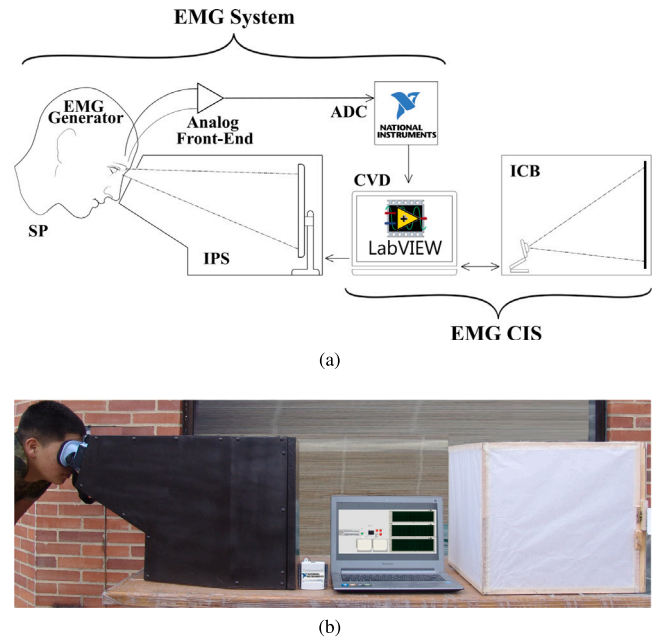

(a)

(b)

Fig. 6. Experimental Setup. (a) Diagram.(b) Photograph.

visual perception. Furthermore, this contribution is the same effect as a pinhole camera, improving the depth of focus and subtly altering lens curvature [21].

The proposed experimental setup allows for the evaluation of the controllability of systems based on superciliary muscle EMG control, such as the one proposed in [10], under controlled conditions. This approach minimizes the number of environmental and physiological variables, as well as their interactions. To ensure consistency, the study imposed restrictions on the age, physical condition, and visual health of the participants. The test group comprised five young university students, ranging in age from 23 to 26 years, who did not have any optical or physical diseases.

3.2. Experimental setup description

An experimental setup was implemented to quantitatively analyze the capability of the SP to control an external optical power device. This setup is depicted in Fig. 6. In the proposed platform, a black-and-white pattern image (Fig. 7) is positioned at a fixed distance from a camera with controllable focus, specifically the Logitech C920 Full HD. The setup is conducted under semi-controlled lighting conditions, with diffuse lighting at approximately 300 lux, adhering to the illuminance level recommended by the IESNA for meeting rooms [41]. The camera's image is then transmitted to a computer, which displays it on a screen. This visual display unit is placed within a matte black box, both on the outside and inside, featuring a visual aperture. The SP observes the image on the screen through the aperture at a constant distance of 55 cm, intentionally chosen to minimize vergence changes. Eye blinkers are used during observation, and the distance is set greater than the SP's minimum focusing distance. The SP may wear corrective glasses if necessary.

The projected image in the IPS may initially be out of focus, prompting the SP to attempt to focus the image by engaging their corrugator muscles, which generates an EMG signal. This signal is detected by the EMG system using an active electrode (specifically, the Z03-003 manufactured by Motions Lab Systems) placed on the muscle. The EMG signal is then processed and transmitted to the EMG CIS system, which controls the focus of the camera located in the image capture box. The captured image pattern is subsequently sent back to
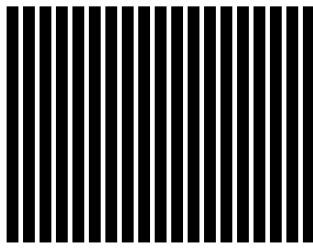
Fig. 7. Selected pattern using in the experimental setup.

the IPS system to close the biofeedback loop. As a result, if the screen image is sharp (indicating successful camera focusing) and the user determines the required optical power of the crystalline lens to focus the screen, the SP perceives a sharp image. This platform effectively decouples camera control from the rest of the optical system, enabling an objective assessment of its controllability.

The EMG signal is captured by the EMG Generator (i.e., electrodes and the SP) and is processed through several stages in the analog front-end and Analog-to-Digital Converter (ADC) system. These stages involve an active electrode, instrumentation amplifier, filter, and isolated amplifier with digital programmable gain. For reducing common noise produced by the 60 Hz power line, we selected the active electrode Z03-003, which provides a voltage gain of 300 V/V and a common mode rejection ratio (CMRR) greater than 100 dB within a Signal Bandwidth of 15 Hz to 2 kHz [42]. The next amplifier stage utilizes an INA128 instrumentation amplifier [43] with a user-selectable gain and a CMRR exceeding 130 dB, effectively maintaining low 60 Hz noise.

The active multistage filter, implemented with OPA2132 operational amplifier [44], is a third-order band-pass filter with a low cutoff frequency of 25 Hz and a high cutoff frequency of 500 Hz. This frequency range aligns with the guidelines of the European organization SENIAM (Surface ElectroMyoGraphy for the Non-Invasive Assessment of Muscles), which recommend low-cut frequencies around 20 Hz and high-cut frequencies up to 1 kHz to mitigate artifacts caused by muscle-skin and electrode-skin motion [45]. Refs. [46,47] support the selection of this frequency range, with [46] suggesting a low-cut frequency of 15–28 Hz for facial muscles and [47] analyzing the spectral density function of the EMG and identifying the relevant frequency range as 8 Hz to 500 Hz.

The active filter also serves as an antialiasing filter for the ADC, which is integrated into the Multifunction I/O Device USB6366 [48] and operates at a sampling frequency of 10 kS/s and 16 bits, as recommended by SENIAM [45]. The isolated amplifier with digitally programmable gain consists of two stages, with the isolated stage utilizing AMC 1200 [49] and the programmable gain stage employing PGA 281 [50].

After the processing of the EMG signal in the analog front-end and Analog-to-Digital Converter (ADC) system, the digital EMG signal is transmitted to the EMG CIS system. The control and visualization device (CVD) encompasses several steps. Firstly, a software-adjustable digital notch filter is employed to further mitigate power line noise. Secondly, to prevent system saturation, the gain of the programmable amplifier is adjusted using the software interface and set below the Maximum Voluntary Contraction (MVC) of the SP. Thirdly, the CVD calculates the Root Mean Square (RMS) of the received digital EMG signal. Fourthly, the CVD establishes a communication link with the camera responsible for capturing the pattern image in the Image Capture Box (ICB). This link serves two purposes: receiving the captured image and adjusting the camera focus based on the RMS value of the digital EMG signal.

Finally, the CVD transmits the image to the IPS system, which comprises an image projection box, a digital screen, eye blinkers,

and the SP. The image projection box isolates the screen projection from external lighting conditions, while the blinkers restrict the SP's peripheral vision. Additionally, the overall process is visualized and stored in a user interface. These functionalities are implemented on a dedicated computer using LabView software.

3.3. Experimental test protocol

To quantitatively validate the control capacity of the SP an experiment was designed to resolve the following question: The SP could control the camera's optical power to focus the projected image. The proposed experiment uses the experimental setup described in Section 3.1 and the protocol detail below:

1. After instructing the SPs to perform the MVC and to minimize EMG signal distortion, it is necessary to adjust the voltage gain of the system to prevent voltage saturation of the amplifiers involved.
2. Locate the 43×28 cm printed pattern (see Fig. 7) at a distance of 25 cm from a camera with a resolution of 430×240 pixels which captures images at 30 frames per second into the image capture box under semi-controlled lighting conditions.
3. Run an auto-focus program and store the Focus Indicator (FI) value, which is a number from 0 to 256 generated by the camera.
4. Install an active electrode pair on the forehead to read the SP EMG activity.
5. Locate the SP in the IP system facing semi-controlled lighting conditions and restricted vision.
6. Begin a training period. This stage of the experiment will last for as long as the volunteer feels comfortable with the overall system, which is limited to one hour.
7. Star the experiment. After a few seconds of observing the focused image, the program abruptly blurs the image on the screen (changes the FI).
8. Sense and store the EMG activity of the SP due to his/her muscular activity.
9. Modify and store the FI based on the sensed EMG activity.
10. Finish the experiment when the FI is set to a value that is equal to or less than the value discovered during the auto-focus procedure.

The experiment was conducted eight times following the adaptation phase, once the test subjects felt comfortable using the camera's control. The final test was excluded to mitigate the potential bias introduced by fatigue. Additionally, the first two tests were excluded from the dataset as they were deemed part of the training phase. Consequently, the analysis focuses exclusively on the normalized results derived from the remaining five tests.

3.4. Experimental waveform description

The typical waveforms of the FI and RMS EMG signals in the experiment are shown in Fig. 8. At time zero, the program rapidly defocuses the image, initiating a delay phase that continues until the SP begins controlling the focus using the RMS EMG signal. This is followed by the set focus phase, where the SP increases its EMG activity to enhance image sharpness. If the SP's EMG activity remains below a certain threshold, the image focus remains constant. The control logic for this process is illustrated in Fig. 9. In this algorithm, the camera focus increases steadily as the EMG activity of the superciliary corrugator muscle exceeds a threshold value, which is set as the 20% MVC RMS value. Setting thresholds below 2.5% MVC RMS presents challenges in detecting changes in the power spectral density function, while excessively high values can lead to subject fatigue [47]. Upon reaching the end of the set focus phase, the SP achieves the sharpest image. Subsequently, the SP maintains low EMG activity briefly in the focus phase before attempting to improve sharpness again in the error focus phase. However, these attempts are unsuccessful because
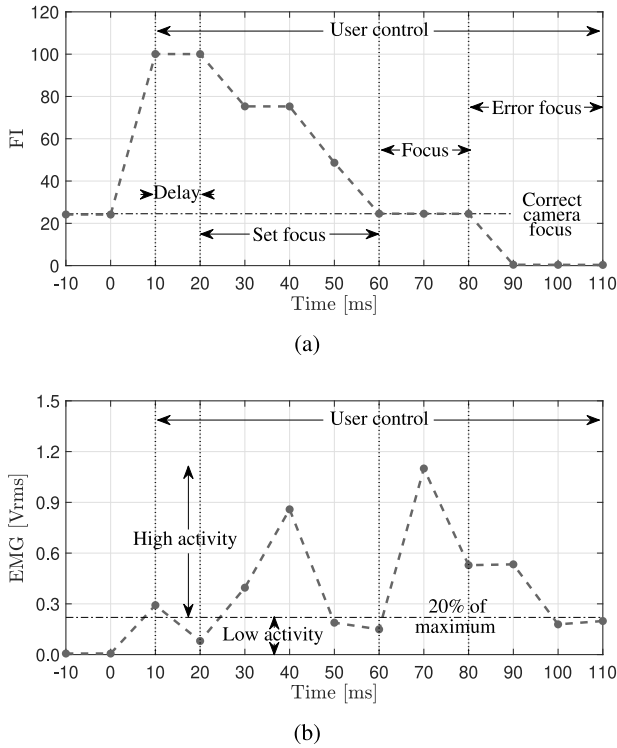
(a)

(b)

Fig. 8. Typical experimental waveforms. (a) Camera Focus Indicator (FI) vs time. (b) Electromyography (EMG) vs time.
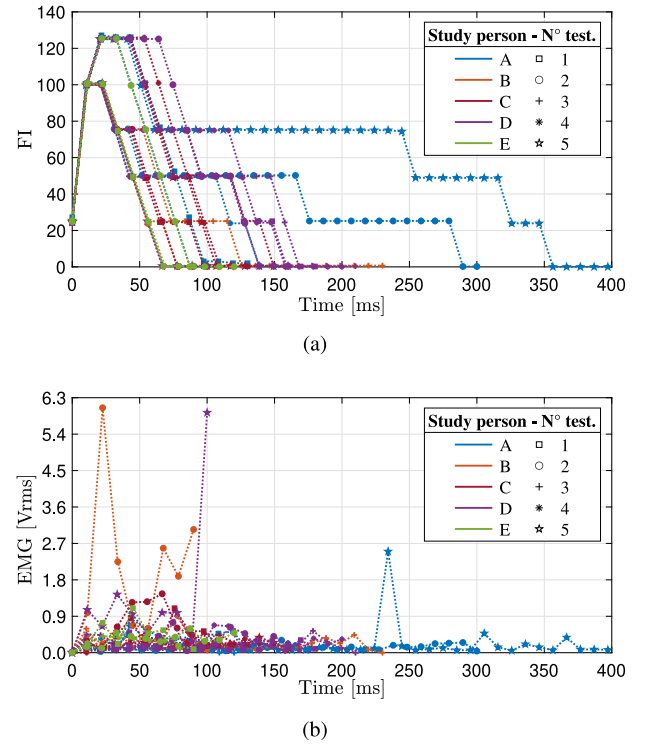

(a)

(b)

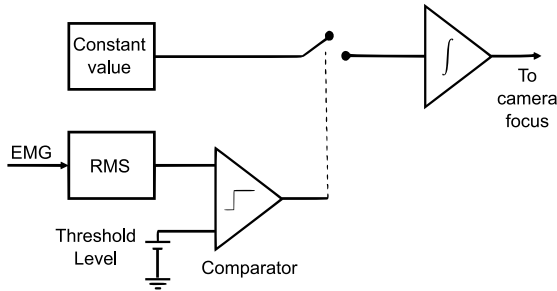**Fig. 10.** Experimental waveforms. (a) FI vs time.(b) EMG vs time.

Fig. 9. Control algorithm of the camera focus.

the system can only correct image focus by increasing the optical power of the tunable lenses, not decreasing it. It is worth noting that the proposed control strategy incorporates an integral action, resulting in a time delay between the FI and EMG waveforms.

4. System results

The experimental waveforms of the FI and RMS EMG signals are presented in Fig. 10. Additionally, Figs. 11 and 12 summarize the resulting statistics, including the mean, maximum, and minimum values of the normalized waveforms, to analyze the main behaviors of the SPs at both individual and overall participant levels. It is worth noting that the camera's focusing time (less than 50 ms) surpasses the human accommodation time (ranging from 400 ms to 1000 ms [7]), which is crucial for interpreting these findings.

The waveform shown in Fig. 10(a) illustrates the consistent improvement in camera focus achieved by the SPs after the training stage. Notably, this improvement is accompanied by significant inter-person variation, which is commonly observed in experiments involving human participants. Furthermore, the typical response time for switching from an unfocused to a focused image ranges from 50 to 350 ms. This

response time aligns with the reported literature on the time required to transition between far and near vision (i.e., 350 ms [7]).

Based on the analysis presented in Fig. 11, it can be observed that SP 1 and SP 4 exhibit a considerable dispersion of data points in comparison to their respective means. This higher dispersion could potentially be attributed to training lag. Furthermore, when considering the mean values of each SP, it is evident that the RMS EMG and the associated focus strategy vary among individuals. For instance, SP 1, SP 2, and SP 4 are characterized by an initial high effort, followed by a brief decrease, and eventually, a final high effort to complete the experiment. However, regardless of these individual variations, all SPs demonstrate the ability to reduce the FI through their control actions, thereby enabling the adjustment of camera focus and enhancing the sharpness of the projected image. This adjustment continues until the final FI matches the value obtained through the camera's autofocus function.

Considering the mean values of the overall SPs in Fig. 12, the person can reduce the FI with their EMG activity using the proposed biofeedback setup. Furthermore, in the control user stage, this activity is characterized by a higher increase at the start of the stage and a constant activity until the end of the test, even after image focus is reached because the SP can only change the focus in one direction.

5. Conclusions

An experimental method for studying and evaluating the controllability of eyeglasses based on biofeedback and tunable lenses was implemented and assessed in this article. Although each volunteer uses a different focusing technique after the training phase, all users were able to control the systems and achieve the setpoint (i.e., a sharp image on the screen). The response time from an unfocused to a focused image was between 50 and 350 ms, which is consistent with the human natural focus times. The proposed experimental setup, as demonstrated in the paper, was very useful for objectively assessing the controllability of systems based on eyeglasses with power controller lenses.
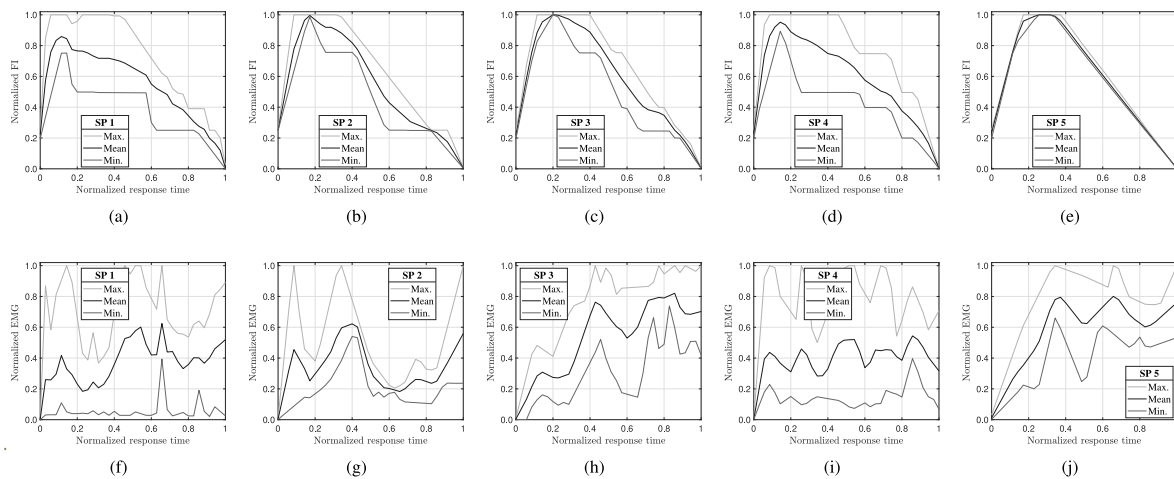
Fig. 11. Experimental Normalized waveforms by person. (a) FI SP 1. (b) FI SP 2. (c)FI SP 3. (d) FI SP 4. (e) FI SP 5. (f) EMG SP 1. (g) EMG SP 2. (h) EMG SP 3. (i) EMG SP 4. (j) EMG SP 5.
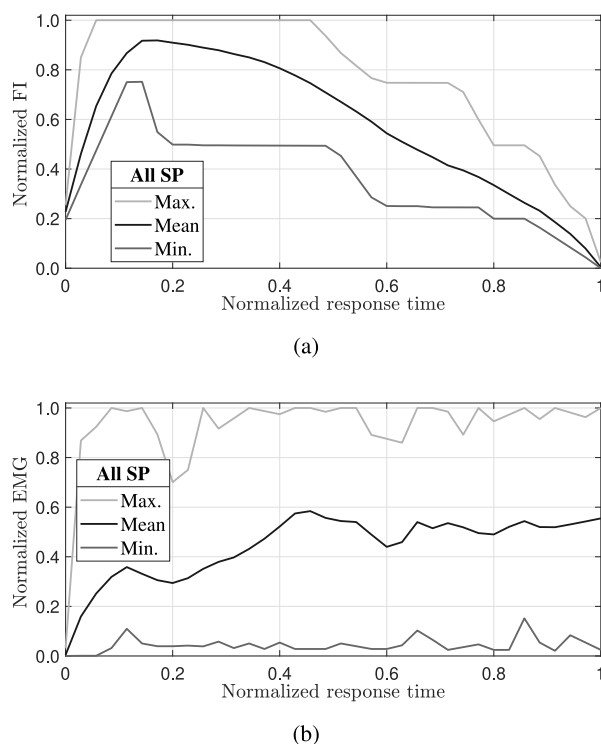

Fig. 12. Overall experimental waveforms. (a) Camera Focus Indicator vs time. (b) Electromyography vs time.

In our future work, we plan to enhance the proposed platform by implementing the following improvements: (1) Adding the capability to adjust the camera's focus in both directions to replicate human vision more accurately. (2) Utilizing a camera to measure the pupil diameter while observing the SP. This measurement will help us to evaluate whether the pupil diameter remains constant due to consistent illumination or if it changes as a result of variations in the contrast of the projected image. (3) Future research endeavors are planned to involve older individuals with presbyopia and/or other visual diseases. This expansion of the participant pool will allow for the investigation of the effects of visual diseases on the controllability of smart eyeglasses based on superciliary muscle EMG control.

Declaration of competing interest

The authors declare that they have no known competing financial interests or personal relationships that could have appeared to influence the work reported in this paper.

Data availability

Data will be made available on request

Declaration of Generative AI and AI-assisted technologies in the writing process

During the preparation of this work the author(s) used [Quillbot, Grammarly and ChatGPT] in order to [enhance its orthography, grammatical style, fluency, coherency, and conciseness]. After using this tool/service, the author(s) reviewed and edited the content as needed and take(s) full responsibility for the content of the publication.

References

[1] M. Katz, P. Kruger, Chapter 33: The human eye as an optical system, in: Duane's Clinical Ophthalmology, Lippincott, Williams & Wilkins, Philadelphia, PA, 2013.

[2] J.D. Silver, D.N. Crosby, G.E. MacKenzie, M.D. Plimmer, Estimating the Global Need for Refractive Correction, Centre for Vision in the Developing World, URL: http://www.icoptix.com/wp-content/uploads/2014/07/Centre-for-Vision-in-Dev-world-Oxford.pdf.

[3] T.R. Fricke, N. Tahhan, S. Resnikoff, E. Papas, A. Burnett, S.M. Ho, T. Naduvilath, K.S. Naidoo, Global prevalence of presbyopia and vision impairment from uncorrected presbyopia: systematic review, meta-analysis, and modelling, Ophthalmology 125 (10) (2018) 1492–1499.

[4] M.U. Karkhanis, C. Ghosh, A. Banerjee, N. Hasan, R. Likhite, T. Ghosh, H. Kim, C.H. Mastrangelo, Correcting presbyopia with autofocusing liquid-lens eyeglasses, IEEE Trans. Biomed. Eng. 69 (1) (2021) 390–400.

[5] N. Padmanaban, R. Konrad, G. Wetzstein, Autofocals: Evaluating gaze-contingent eyeglasses for presbyopes, Sci. Adv. 5 (6) (2019) eaav6187.

[6] N. Hasan, M. Karkhanis, F. Khan, T. Ghosh, H. Kim, C.H. Mastrangelo, Adaptive optics for autofocusing eyeglasses, in: Imaging and Applied Optics 2017 (3D, AIO, COSI, IS, MATH, PcAOP), Optica Publishing Group, 2017, p. AM3A.1, http://dx.doi.org/10.1364/AIO.2017.AM3A.1, URL: http://opg.optica.org/abstract.cfm?URI=AIO-2017-AM3A.1.

[7] J. Jarosz, N. Molliex, G. Chenon, B. Berge, Adaptive eyeglasses for presbyopia correction: an original variable-focus technology, Opt. Express 27 (8) (2019) 10533–10552.

[8] J. Mompeán, J.L. Aragón, P. Artal, Portable device for presbyopia correction with optoelectronic lenses driven by pupil response, Sci. Rep. 10 (1) (2020) 1–9.

[9] T. Fujita, S. Sato, M. Idesawa, A gazing point distance detection system for accommodation assisting glasses, in: SENSORS, 2002 IEEE, Vol. 2, IEEE, 2002, pp. 905–910.

[10] R. Linero-Ramos, G. Yamhure-Kattah, J. Gomez-Rojas, Evaluation of the improvement in visual acuity using electronic system biofeedback, J. Xi'an Univ. Archit. Technol. 12 (7) (2020) 1401–1411.

[11] T. Inoue, VDT eyeglasses—multifocal lenses for near distance use, Displays 23 (1–2) (2002) 11–16.

[12] G.A. da Silva, P.A. Nogueira, R. Rodrigues, Multimodal vs. unimodal biofeedback in videogames: an empirical player study using a first-person shooter, in: 2014 9th Iberian Conference on Information Systems and Technologies, CISTI, IEEE, 2014, pp. 1–6.

[13] C.A. Castillo, B. Gayed, C. Pedrono, K.J. Ciuffreda, J.L. Semmlow, T.L. Alvarez, The transient component of disparity vergence maybe an indication of progressive lens acceptability, in: 2006 International Conference of the IEEE Engineering in Medicine and Biology Society, IEEE, 2006, pp. 5687–5690.

[14] T.L. Alvarez, S. Han, C. Kania, E. Kim, O. Tsang, J.L. Semmlow, B. Granger-Donetti, C. Pedrono, Adaptation to progressive lenses by presbyopes, in: 2009 4th International IEEE/EMBS Conference on Neural Engineering, IEEE, 2009, pp. 143–146.

[15] J.F. Algorri, D.C. Zografopoulos, V. Urruchi, J.M. Sánchez-Pena, Recent advances in adaptive liquid crystal lenses, Crystals 9 (5) (2019) 272.

[16] M. Rosenfield, Computer vision syndrome: a review of ocular causes and potential treatments, Ophthalmic Physiol. Opt. 31 (5) (2011) 502–515.

[17] A. Kuwahara, K. Nishikawa, R. Hirakawa, H. Kawano, Y. Nakatoh, Eye fatigue estimation using blink detection based on Eye Aspect Ratio Mapping(EARM), Cogn. Robotics 2 (2022) 50–59.

[18] H. Richter, T. Bänziger, S. Abdi, M. Forsman, Stabilization of gaze: A relationship between ciliary muscle contraction and trapezius muscle activity, Vis. Res. 50 (23) (2010) 2559–2569, Vision Research Reviews.

[19] W.N. Charman, The eye in focus: accommodation and presbyopia, Clin. Exp. Optom. 91 (3) (2008) 207–225.

[20] S.K. Gupta, S. Aparna, Effect of yoga ocular exercises on eye fatigue, Int. J. Yoga 13 (1) (2020) 76–79.

[21] K.J. Ciuffreda, Accommodation, the Pupil, and Presbyopia, Butterworth Heineman, 2006, pp. 93–144.

[22] M.U. Karkhanis, A. Banerjee, C. Ghosh, R. Likhite, E. Pourshaban, H. Kim, D.A. Meyer, C.H. Mastrangelo, Compact models of presbyopia accommodative errors for wearable adaptive-optics vision correction devices, IEEE Access 10 (2022) 68857–68867.

[23] K.B. Wolf, Geometric Optics on Phase Space, Springer Science & Business Media, 2004.

[24] A. Prado Montes, Á. Morales Caballero, J.N. Molle Cassia, Síndrome de Fatiga ocular y su relación con el medio laboral, Med. Seguridad Del Trab. 63 (249) (2017) 345–361.

[25] T. Wang, The review of Biofeedback and its mechanism, Med. Inf. 15 (2002) 610–614.

[26] R. Li, D.T. Lai, W. Lee, A survey on biofeedback and actuation in wireless body area networks (WBANs), IEEE Rev. Biomed. Eng. 10 (2017) 162–173.

[27] M. Semprini, A.V. Cuppone, I. Delis, V. Squeri, S. Panzeri, J. Konczak, Biofeedback signals for robotic rehabilitation: Assessment of wrist muscle activation patterns in healthy humans, IEEE Trans. Neural Syst. Rehabil. Eng. 25 (7) (2017) 883–892.

[28] L. Carvalho, H. Albuquerque, C. Pontes, M. Maia, D. Mangueira, L. Batista, Computerized biofeedback tool: application in electromyogram-biofeedback, in: Proceedings of the 25th Annual International Conference of the IEEE Engineering in Medicine and Biology Society (IEEE Cat. No.03CH37439), Vol. 2, 2003, pp. 1609–1612 Vol.2, http://dx.doi.org/10.1109/IEMBS.2003.1279674.

[29] D. Shuhan, H. Tanabe, Y. Morita, Z. Peichen, Effect of introducing EMG biofeedback to a finger extensor facilitation training device for hemiplegic patients after strokes, in: 2019 19th International Conference on Control, Automation and Systems, ICCAS, 2019, pp. 184–187, http://dx.doi.org/10.23919/ICCAS47443.2019.8971742.

[30] Y. Fang, Z.F. Lerner, Feasibility of augmenting ankle exoskeleton walking performance with step length biofeedback in individuals with cerebral palsy, IEEE Trans. Neural Syst. Rehabil. Eng. 29 (2021) 442–449.

[31] J. Ling, J.C. Hong, Y. Hayashi, K. Yasuda, Y. Kitaji, H. Harashima, H. Iwata, A haptic-based perception-empathy biofeedback system with vibration transition: Verifying the attention amount, in: 2020 42nd Annual International Conference of the IEEE Engineering in Medicine and Biology Society, EMBC, 2020, pp. 3779–3782, http://dx.doi.org/10.1109/EMBC44109.2020.9176213.

[32] T. Oku, S. Furuya, A novel vibrotactile biofeedback device for optimizing neuromuscular control in piano playing, in: 2019 IEEE Conference on Virtual Reality and 3D User Interfaces, VR, 2019, pp. 1554–1555, http://dx.doi.org/10.1109/VR.2019.8797765.

[33] Q. Zhu, X.l. Kong, Y.y. Xie, The influence of biofeedback on respiratory training effect, in: 2012 International Conference on Systems and Informatics, ICSAI2012, 2012, pp. 1067–1071, http://dx.doi.org/10.1109/ICSAI.2012.6223218.

[34] W. Sangngoen, W. Sroykham, S. Khemthong, W. Jalayondeja, Y. Kajornpredanon, S. Thanangkul, Effect of EMG biofeedback on muscle activity in computer work, in: The 5th 2012 Biomedical Engineering International Conference, 2012, pp. 1–4, http://dx.doi.org/10.1109/BMEiCon.2012.6465453.

[35] An application of bio-feedback in the rehabilitation of the blind, Applied Ergon. 11 (1) (1980) 31–33.

[36] B.M. Maarsingh, J. Bos, C.F. Van Tuijn, S.B. Renard, Changing stress mindset through stressjam: A virtual reality game using biofeedback, Games Health J. 8 (5) (2019) 326–331.

[37] M. van Rooij, A. Lobel, O. Harris, N. Smit, I. Granic, DEEP: A biofeedback virtual reality game for children at-risk for anxiety, in: Proceedings of the 2016 CHI Conference Extended Abstracts on Human Factors in Computing Systems, in: CHI EA '16, Association for Computing Machinery, New York, NY, USA, 2016, pp. 1989–1997, http://dx.doi.org/10.1145/2851581.2892452.

[38] R. Blendowske, Unaided visual acuity and blur: a simple model, Optom. Vis. Sci. 92 (6) (2015) e121–e125.

[39] B. Bhattacharyya, D. Bhattacharya, Textbook of Visual Science and Clinical Optometry, Jaypee Bros. Medical Publishers, 2009.

[40] W.J. Benjamin, Borish's Clinical Refraction-E-Book, Elsevier Health Sciences, 2006.

[41] A. Fajardo Jaimes, F. Rangel de Sousa, Simple modeling of photovoltaic solar cells for indoor harvesting applications, Sol. Energy 157 (2017) 792–802.

[42] Datasheet Z03 EMG preamplifier, 2023, https://www.motion-labs.com/prod_preamp.html#Z03. (Accessed 21 May 2023).

[43] Datasheet INA128, 2023, https://www.ti.com/product/es-mx/INA128. (Accessed 21 May 2023).

[44] Datasheet OPA2132, 2023, https://www.ti.com/lit/ds/symlink/opa2132.pdf. (Accessed 21 May 2023).

[45] D. Stegeman, H. Hermens, Standards for suface electromyography: The European project surface emg for non-invasive assessment of muscles (SENIAM), 2007, https://citeseerx.ist.psu.edu/document?repid=rep1&type=pdf&doi=b280c4751a2658380a77052b0aab7929e6943a57. (Accessed 21 May 2023).

[46] C.J. De Luca, L.D. Gilmore, M. Kuznetsov, S.H. Roy, Filtering the surface EMG signal: Movement artifact and baseline noise contamination, J. Biomech. 43 (8) (2010) 1573–1579.

[47] D. Roman-Liu, M. Konarska, Characteristics of power spectrum density function of EMG during muscle contraction below 30% MVC, J. Electromyography Kinesiol. 19 (5) (2009) 864–874.

[48] Datasheet USB-6366, 2023, https://www.ni.com/docs/en-US/bundle/pxie-usb-6366-specs/page/specs.html. (Accessed 21 May 2023).

[49] Datasheet AMC1200, 2023, https://www.ti.com/lit/ds/symlink/amc1200.pdf?ts=1686081409697. (Accessed 21 May 2023).

[50] Datasheet PGA281, 2023, https://www.ti.com/lit/ds/symlink/pga281.pdf?ts=1686032914310. (Accessed 21 May 2023).